International Journal of Infectious Diseases 171 (2026) 108973

Contents lists available at ScienceDirect

International Journal of Infectious Diseases

journal homepage: www.elsevier.com/locate/ijid

Vagal cholinergic denervation of the gastric mucosa in Long-COVID-19: *In vivo* evidence of structural autonomic dysfunction

Domenico Acanfora[1,*], Maria Nolano[2,3], Chiara Acanfora[4], Camillo Colella[1], Vincenzo Provitera[3], Giuseppe Caporaso[3], Giuseppe Rengo[5,6], Raffaele Antonelli Incalzi[7], Gerardo Casucci[1]

[1] *Department of Internal Medicine, San Francesco Hospital, Telese Terme, Italy*
[2] *Department of Neurosciences, Reproductive Sciences and Odontostomatology, University of Naples Federico II, Naples, Italy*
[3] *Neurology Department, Skin Biopsy Laboratory, Istituti Clinici Scientifici Maugeri IRCCS, Telese Terme, Italy*
[4] *Vascular and Interventional Radiology Unit, Azienda Ospedaliera Universitaria San Giovanni Di Dio e Ruggi d'Aragona, University of Salerno, Salerno, Italy*
[5] *Department of Translational Medical Sciences, University of Naples Federico II, Naples, Italy*
[6] *Istituti Clinici Scientifici Maugeri, IRCCS di Telese Terme, Telese Terme, Italy*
[7] *Unit of Geriatrics, Policlinico Universitario Campus Bio-Medico di Roma, Rome, Italy*

ARTICLE INFO

Article history:
Received 22 April 2026
Revised 6 July 2026
Accepted 8 July 2026

Keywords:
Long-COVID-19
Autonomic dysfunction
Vagus nerve
Gastric innervations
HRV

ABSTRACT

Objectives: Dysautonomia has been increasingly recognized as a key feature of Long-COVID-19, potentially contributing to persistent gastrointestinal and systemic symptoms. Reduced vagal activity observed in these patients may reflect structural damage to autonomic fibers. We hypothesized that dysautonomic manifestations in Long-COVID-19 are associated with impaired cholinergic innervation of the gastric mucosa.

Methods: We conducted a case–control study including 12 patients with Long-COVID-19 and 8 control subjects undergoing routine gastroscopy. Gastric mucosal biopsies were analyzed using immunohistochemistry with the pan-neuronal marker protein gene product 9.5 (PGP 9.5) and vasoactive intestinal peptide (VIP) as a marker of cholinergic fibers. Nerve fiber density was quantified in both fundus and antrum samples.

Results: Compared with controls, Long-COVID-19 patients exhibited a significant reduction in mucosal innervation density: 2.1 vs 3.9 nm/µm³ ($P < 0.01$) in the fundus and 1.9 vs 3.9 nm/µm³ ($P < 0.05$) in the antrum. The reduction in cholinergic innervation was more pronounced in the fundus ($P < 0.01$) and also evident in the antrum ($P = 0.01$). Gastric nerve density correlated with HRV parameters (LF/HF ratio: $R = 0.50$, $P < 0.05$) and NT-proBNP levels ($R = 0.52$, $P < 0.01$).

Conclusions: Patients with Long-COVID-19 exhibit reduced gastric mucosal cholinergic innervation. This structural autonomic impairment may represent an anatomical substrate underlying dysautonomia in Long-COVID-19.

© 2026 The Authors. Published by Elsevier Ltd on behalf of International Society for Infectious Diseases. This is an open access article under the CC BY-NC-ND license (http://creativecommons.org/licenses/by-nc-nd/4.0/)

Introduction

Since the end of 2019, a coronavirus pandemic (SARS-CoV-2), responsible for severe acute respiratory syndrome, has spread worldwide. This pandemic, due to the spread of SARS-CoV-2, is similar to two previous human coronavirus (HCoV) outbreaks, acute and severe respiratory syndrome (SARS) and Middle Eastern respiratory syndrome (MERS) [1]. SARS-CoV-2 has spread far more quickly and is more contagious than the other two types of HCoVs. All these outbreaks are characterized by respiratory symptoms ranging from sore throat, cough, and dyspnea to acute respiratory distress syndrome (ARDS) [2]. In the acute phase, SARS-CoV-2 penetrates through a link with the angiotensin-converting enzyme 2 (ACE2) receptors [3]. In infected individuals, SARS-CoV-2 invasion is ubiquitous as ACE2 receptor is expressed in all organs and systems.

There is consolidated evidence that SARS-CoV-2 mainly affects the respiratory and cardiovascular systems. Nevertheless, it can be associated with, neurological, and gastrointestinal symp-

* Corresponding author.
E-mail address: domenico.acanfora29@gmail.com (D. Acanfora).

https://doi.org/10.1016/j.ijid.2026.108973
1201-9712/© 2026 The Authors. Published by Elsevier Ltd on behalf of International Society for Infectious Diseases. This is an open access article under the CC BY-NC-ND license (http://creativecommons.org/licenses/by-nc-nd/4.0/)

toms [4]. The involvement of the nervous system (both central and peripheral) is common in patients with coronavirus disease 2019 (COVID-19) and the finding of elevated plasmatic levels of proteins expressing neural damage such as neurofilament light chain protein (NfL), and glial fibrillary acidic protein (GFAp), demonstrate the presence of an impairment of the nervous system in COVID-19 patients [5,6]. Nervous system manifestations have been reported in approximately 37% of COVID-19 patients, often in the early stages of the disease and sometimes even before the occurrence of respiratory symptoms [7]. Early symptoms include anosmia, ageusia, myalgia, cognitive fog, anxiety, headache, depression, hallucinations and other psychiatric symptoms [8]. However, the pathophysiology of neurological manifestations in patients with COVID-19 remains controversial.

Neurological symptoms have been linked to COVID-19 through various mechanisms, such as neuroinvasion, vascular inflammation, and the blood–brain barrier breakdown. Some authors believe that neurological symptoms may be initiated by a direct damage caused by COVID-19 to the olfactory pathways and maintained by the centripetal spread of the disease to central nervous system structures. Alternatively, the virus may reach the central nervous system via the trigeminal nerve after coming into contact with the ocular conjunctiva [9,10]. Other authors correlate the clinical manifestations of patients with COVID-19 and Long-COVID-19 to direct involvement of the vagus nerve (VN) [6,11–13]. It is a mixed nerve with 20% efferent fibers and 80% afferent fibers and is an important component of the parasympathetic branch of the autonomic nervous system (ANS) [14] that innervates the respiratory system, heart, digestive system, kidneys, bladder, uterus and testicles. Therefore, VN may represents a large route of virus translocation from periphery to the central nervous system.

Long-COVID-19 refers to the signs and symptoms that continue or develop after the acute COVID-19 phase and is characterized by a proinflammatory, procoagulative state. Patients who have recovered from acute COVID-19 have a higher risk of rehospitalization, multiorgan dysfunction, and mortality [15,16].

In Long-COVID-19, a dysfunction of the ANS has been reported [11] that can possibly be accounted for some of the extrarespiratory late manifestations of SARS-CoV-2 infection [4]. Immunohistochemical analysis of autonomic innervation has been largely used in recent decades to study normal autonomic innervation of end organs and to characterize peripheral involvement of adrenergic and cholinergic systems in different pathological conditions in humans [17–21]. Due to the availability of tissues, most related work has been performed by processing skin samples [17,18]. However, the technique has been applied to study visceral autonomic innervation of epicardial adipose tissue and myocardium [19,20] and of gastrointestinal mucosa [21].

To test the occurrence and extent of autonomic involvement in Long-COVID-19 patients, we performed a power spectral analysis of heart rate variability (HRV) via 24-hour 12-lead ECG recording in patients and controls. We also performed histological examination of the nerves in the mucosal layer of the gastrointestinal tract. We chose to study the stomach mucosa because this tissue can be safely acquired via standard biopsy techniques during routine endoscopy. We also hypothesize that there is a relationship between gastric mucosal nerve fiber density and the symptoms, procoagulative state and impairment of vagal activity associated with Long-COVID-19.

Therefore, we will correlate autonomic nerve density with clinical characteristics and HRV parameters in Long-COVID-19 patients.

Materials and methods

Patients

We consecutively enrolled 12 patients admitted to our Department from 12 July 2021 to 23 February 2024 with persistent symptoms, including dyspnea, fatigue, chest pain, joint pain, myalgia, cough, headache, loss of appetite, dyspepsia, nausea, vomiting and bloating following SARS-CoV-2 infection; symptoms persisted for more than 12 weeks, fulfilling the criteria for the diagnosis of Long-COVID-19 syndrome [22]. Eight patients without previous SARS-CoV-2 infection who underwent screening gastroscopy for dyspepsia composed our control population (Controls). All Long-COVID-19 and Controls patients had received 3 doses of BNT162b2/COMIRNATY vaccine.

The exclusion criteria were as follows: permanent atrial fibrillation (PAF), ventricular ectopic beats >600/24 h, the presence of a pacemaker or implantable cardioverter defibrillator, heart failure, clotting disorders, diabetes, kidney failure, liver failure, dysthyroidism, dysendocrinopathy, alcohol abuse, active cancer under chemotherapy, peripheral neuropathy or conditions potentially affecting the peripheral nervous system.

This study was performed in accordance with the ethical guidelines of the 1975 Declaration of Helsinki and was approved by the local Institutional Review Board (22 March 2021) of the San Francesco Hospital of Telese Terme (BN). All procedures complied with the ethical standards of institutional and national research. Informed consent was obtained from all participants included in the study.

Study protocol

All patients were clinically stable and in sinus rhythm. Patients had been on a stable pharmacological regimen for at least 2 weeks before hospital admission. Therefore, all patients were on optimal medical therapy at the time of admission. After admission, all patients provided their demographic data, medical history, vital signs, clinical and anthropometric data, neurologic examination results, blood chemistry test results, and HRV assessment via 24-h ECG, as previously described [13]. In short, patients were applied a portable twelve-channel tape recorder, processed by a DM Software Inc. version 12.5.0078a, (Diagnostic Monitoring Software P.O. Box 3109; 209 Kingsbury Grade, #3; Stateline, NV 89449, USA) for 24-h ECG recordings which were uploaded to the PC. After scanning, any artifacts were removed and the recordings were analyzed with the 24-h ECG software at a sampling frequency of 128 Hz. At admission, all patients underwent preparation of the skin, then self-adhesive electrodes were placed in the usual positions for twelve-lead ECG monitoring, and recording was started between 9:00 and 9:30 a.m. During recording, patients were allowed to be standing or sitting next to their beds, while no other activities were allowed. The 24-h ECG monitoring software documented HRV parameters automatically as numerical data. Patients were considered eligible for the study if their recordings had at least 12 h of analyzable intervals between consecutive R peaks. Furthermore, the recording period was analyzed if it included at least half of the night-time (from 00:00 a.m. through to 5:00 a.m.) and half of the daytime (from 7:30 a.m. through to 11:30 p.m.) [23]. The labeling of each beat as normal or aberrant was done according to recognition by the algorithm for tape analysis and based on an investigator's check. Time-domain measures (SDNN, SDANN, ASDNN, rMSSD, pNN50) and frequency-domain measures (VLF, LF, HF, LF/HF) were calculated for HRV assessment. Power spectral density (PSD) was estimated using the Blackman–Tukey method in all accepted segments after linear trend removal. PSD is a highly reproducible tool used to assess the functional balance be-

tween parasympathetic and sympathetic domains of the autonomic nervous system activity and to break down the total variation of a data series into its frequency components. The total power (TP) and the power in the very low frequency band (VLF, 0.01-0.04 Hz), low frequency band (LF, 0.04-0.15 Hz), and high frequency band (HF, 0.15-0.45 Hz) were then computed by numerical integration of the spectral density function. The analysis took into consideration only normalized TP, VLF, LF, and HF values which were expressed as natural logarithms (ln ms^2) to minimize skewness. The LF/HF ratio was also calculated. Based on the ACC/AHA/ESC consensus [23], the following HRV parameters were defined: HF component, mainly reflecting the efferent vagal activity; LF component, which is mediated by efferent vagal and sympathetic activity; LF/HF ratio, a measure of sympatho/vagal balance; VLF component, which reflects neuroendocrine and thermoregulatory influences mediated mainly by the sympathetic system [24,25]. The time-domain parameters, which are most commonly used, were derived from normal RR intervals (NN). These include the square root of the mean squared differences of successive RR intervals (RMSSD) that is associated with respiratory effects on heart rate and is modulated by both parasympathetic and sympathetic activity, with the proportion derived by dividing the number of interval differences of successive NN intervals greater than 50 ms (NN50) by the total number of NN intervals (pNN50) reflects rapid adjustments, and the standard deviation of NN (SDNN) expresses overall HRV regulation.

Upper endoscopy was performed under conscious sedation following overnight fasting. Biopsies from the gastric mucosa were performed via gastrointestinal endoscopy from the proximal (fundus) and distal (antrum) parts of the stomach (Supplementary Figure 1).

The same endoscopist performed all the biopsies for controls and patients in a blinded fashion.

An additional skin biopsy from the leg was performed to assess intraepidermal nerve fiber density (IENF) for comparison with mucosal innervation. The density of IENF was calculated according to international guidelines [26].

The leg biopsies were collected by a 3-mm disposable punch. All biopsies were fixed in Zamboni solution for 5 hours and then cryopretected with a solution of polyvinylpyrrolidone. All the biopsies were immunostained and analyzed at the Skin Biopsy Lab of the ICS Maugeri IRCCS of Telese Terme. Tissue samples were cut with a sliding microtome at 100 µm for the gastric mucosa and 50 µm for the leg. Specimens were processed via indirect immunofluorescence using a panel of primary antibodies including pan-neuronal marker protein gene product 9.5 (PGP 9.5) for "total" nerve fibers, vasoactive intestinal peptide (VIP) for autonomic cholinergic fibers, collagen type IV (COL-IV) for glandular structures, blood vessels and thin muscle layers separating mucosa from sub-mucosa and ulex europaeus agglutinin I (ULEX) an agglutinin that binds to epithelia and endothelia. To characterize the immunohistochemical phenotype of mucosa nerve fibers we assessed, in a sub-group of subjects, the colocalization of VIP with adrenergic (DBH), sensory (Sub-P) and pan-neuronal (PGP 9.5) markers. Primary antibodies were visualized using species-specific secondary antibodies coupled with the fluorophores Cy2, Cy5 and Cy3 (Supplementary Table 1) [27].

We acquired a total of 248 digital images from the fundus and antrum using a non-laser confocal microscope (Axioimager M.2 with Apotome2, Zeiss, Jena, Germany). The density of nerve fibers in the fundus and antrum was quantified with Neurolucida 360 software (MBF Bioscience, Inc., Williston, VT, USA) that performs accurate reconstruction of neuronal structures. Briefly, the software, based on a 3D tracing method, uses algorithms to trace axons point by point. The software only takes in account fluorescence morphologically compatible with axon structure in terms of thickness, continuity, curvature, direction and brightness and creates a 3D map of the nerves included within the region of interest. Finally, the software calculates the length of PGP 9.5 and VIP nerves per volume of tissue ($nm/\mu m^3$) (Supplementary Figure 1) [27]. For the quantitative evaluation, sample size analysis was based on the mean and standard deviation of pan-neuronal fundus nerve density observed in the control group considering a minimum difference of 1 $nm/\mu m^3$ of nerve length. The calculated sample size was of 10 patients to achieve a statistical significance.

All the procedures for quantifying nerve fibers were executed by an operator blinded to the diagnosis.

Statistical analysis

To test whether variables were normally distributed, we used the Shapiro-Wilk test. Differences between the Long-COVID-19 patients and the Control group were evaluated by the Mann–Whitney test or t-test, as appropriate. Pearson or Spearman tests were used, as appropriate, to assess possible correlations between clinical, morphological, and demographic data. We performed power and sample-size analysis using the "onemean" command of Stata software and assuming an error alpha equal to 5% and a study power of 80%. The data are presented as the mean ± SD or median and interquartile range (IQR) based on the distribution of the values.

Results

The demographic and clinical data, neurological examination findings and laboratory data of the patients in the study groups are summarized in Table 1 and Supplementary Table 2.

Among the Long-COVID-19 patients, 66% (8/12) reported orthostatic intolerance, 66% (8/12) reported vasomotor symptoms, 25% (3/12) reported hyperhidrosis, and 42% (5/12) reported gastrointestinal symptoms, while in the Control group 25% (2/8) reported vasomotor symptoms, 25% (2/8) reported gastrointestinal symptoms and none reported orthostatic intolerance or hyperhidrosis. No subjects from the two groups reported urinary or pupillomotor dysfunction.

Samples of gastric biopsies from Long-COVID-19 patients were obtained 21.0 ± 10.2 (range 12-52) weeks after nasopharyngeal swab negativity. Endoscopy revealed that the stomach mucosa appeared normal in Control and Long-COVID-19 patients. Hematoxylin-eosin (H&E) staining of histological sections of the gastric mucosa for *Helicobacter pylori* was negative in Controls and Long-COVID-19 patients.

In controls the gastric mucosa, as observed by fluorescence microscopy, appeared to be richly innervated with both PGP 9.5 and VIP staining. Fibers from a rich submucosal neural plexus reached the apex of the papillae. In patient samples, the innervation was poorer and irregular. The submucosal plexus was less rich, fibers in the mucosal papillae were sparse, and most of the fibers did not reach the apex of the papillae (Figure 1).

In both antrum and fundus, sensory (Sub-P-ir) and noradrenergic (DBH-ir) nerve fibers were scarcely represented with no difference between patients and controls. They were located in muscularis mucosa and did not colocalize with VIP that, as it happens in the skin, also in the gastric mucosa colocalize with cholinergic fibers as demonstrated by its co-expression with ChAT [28]. In our samples most of the VIP-ir fibers showed colocalization with PGP 9.5 (Supplementary Figure 3).

Quantitative assessment of mucosal innervation demonstrated that the density of PGP-ir nerves in Long-COVID-19 patients was lower than that in Controls ($P < 0.01$) in the fundus and in the antrum ($P < 0.05$). The loss of VIP-ir (cholinergic) nerves was even more evident in the fundus ($P < 0.01$). This loss, although to a

Table 1
Clinical characteristics of the study population.

	Controls	Long-COVID-19	P
Demographics			
Sex (male/female)	5/3	6/6	>0.05
Age, years	54.3 ± 17.9	56.5 ± 16.2	>0.05
Weight, kg	82.5 ± 18.1	77.1 ± 18.4	>0.05
Height, cm	172.8 ± 10.6	168.5 ± 11.1	>0.05
Body mass index, kg/m^2	27.7 ± 4.2	27.2 ± 5.1	>0.05
Preexisting conditions in the last year			
Chronic neurological disease (yes/no)	2/8 (25.0%)	1/12 (8.33%)	>0.05
Hypertension (yes/no)	1/8 (12.5%)	4/12 (33.34%)	>0.05
Mental health conditions (yes/no)	1/8 (12.5%)	3/12 (25%)	>0.05
Covid-19 history			
Time after covid immunization (months)	NA	4.8 ± 3.0	NA
Hospitalization by COVID-19 (days of hospitalization)	NA	5/12 (12.3 ± 15.3)	NA
Autonomic symptoms			
Orthostatic intolerance	0/8 (0.0%)	8/12 (66.0%)	<0.01
Vasomotor dysfunction	2/8 (25.0%)	8/12 (66.0%)	>0.05
Secretomotor dysfunction	0/8 (0.0%)	3/12 (25.0%)	>0.05
Gastrointestinal dysfunction	2/8 (25.0%)	5/12 (42.0%)	>0.05
Urinary dysfunction	0/8 (0.0%)	0/8 (0.0%)	NA
Pupillomotor dysfunction	0/8 (0.0%)	0/8 (0.0%)	NA
Therapies			
ACE-I/ARB/ARNIs (yes/no)	1/8 (12.5%)	4/12 (33.3%)	>0.05
Beta-blockers (yes/no)	2/8 (25.0%)	2/12 (16.7%)	>0.05
ASA (yes/no)	1/8 (12.5%)	2/12 (16.7%)	>0.05
Diuretics (yes/no)	0/8 (0.0%)	3/12 (25.0%)	>0.05
Anticoagulants (yes/no)	0/8 (0.0%)	3/12 (25.0%)	>0.05
Neurologic sensory examination			
Vibration (normal/abnormal)	8/0 (100.0%)	12/0 (100.0%)	NA
Pinprick (normal/abnormal)	8/0 (100.0%)	12/0 (100.0%)	NA
Light touch (normal/abnormal)	8/0 (100.0%)	12/0 (100.0%)	NA
Position sense (normal/abnormal)	8/0 (100.0%)	12/0 (100.0%)	NA
Motor examination, strength (score 0-5)	4.2 ± 0.8	3.5 ± 0.5	>0.05
Abnormal achilles reflex (normal/abnormal)	8/0 (100.0%)	12/0 (100.0)	NA

ACE-I = angiotensin-converting enzyme inhibitor; ARB = angiotensin receptor blocker; ARNIs = angiotensin receptor neprilysin inhibitors; ASA = acetylsalicylic acid; NA = not applicable.
Data are reported as mean ± standard deviation and percentage when applicable.

lesser extent, was also observed in the antrum ($P < 0.01$) (Figure 1 and 2A).

Intraepidermal nerve fiber density was not different between the 2 groups of patients ($P > 0.05$), and no correlation was found between IENF and mucosal nerves. Data on mucosal and cutaneous innervation are detailed in Table 2.

Compared to Controls, Long-COVID-19 patients had impaired cardiovascular autonomic control, as assessed by HRV (LF/HF ratio = 1.7 ± 0.2 vs 1.1 ± 0.1, $P < 0.01$); higher D-dimer levels, 796.6 ± 167.7 vs 348.7 ± 78.1, $P < 0.01$ (suggesting a higher risk of thromboembolism); and higher NT-proBNP levels, 646.4 ± 307.9 vs 258.6 ± 172.1, $P < 0.01$, a marker of heart failure. Details on recorded parameters of HRV are reported in Table 3.

The gastric mucosa nerve density correlated with the HRV (LF/HF $R = 0.50$, $P < 0.05$, Coef. −2.40), NT-proBNP level ($R = 0.52$, $P < 0.01$,) and D-dimer level ($R = 0.61$, $P < 0.01$,) (Figure 2B to 2D).

Discussion

The present study provides, to our knowledge, the first *in vivo* morphological evidence of selective cholinergic denervation within the gastric mucosa of patients with Long-COVID-19. By integrating histological findings with functional autonomic assessment, our results support the existence of a structural–functional impairment of the autonomic nervous system, with predominant involvement of the parasympathetic (vagal) pathway.

A central finding of this study is the marked reduction in mucosal nerve fiber density, particularly affecting cholinergic (VIP-positive) fibers. This observation is of particular relevance, as it suggests that autonomic dysfunction in Long-COVID-19 is not merely a functional disturbance but may reflect an underlying structural lesion. The preferential involvement of cholinergic fibers further points to a selective vulnerability of the parasympathetic system, consistent with the clinical phenotype characterized by reduced vagal tone and sympathovagal imbalance.

Importantly, the observed structural alterations were significantly associated with functional indices of autonomic regulation, including HRV parameters, NT-proBNP levels, and D-dimer concentrations. This convergence of morphological and physiological data strengthens the hypothesis that vagal impairment represents a central mechanism linking local neural damage to systemic manifestations. In particular, the correlation with HRV indices reinforces the interpretation of reduced parasympathetic activity, while the association with biomarkers of cardiovascular stress and coagulation suggests a broader systemic impact of autonomic disruption.

The absence of significant differences in intraepidermal nerve fiber density between patients and controls provides an additional layer of insight. Unlike conditions such as diabetic neuropathy, in which somatic and autonomic fibers are concomitantly affected [21], our findings suggest a more selective involvement of visceral autonomic pathways. This selective vulnerability may reflect specific mechanisms of SARS-CoV-2 neurotropism or immune-mediated injury targeting the vagus nerve and its peripheral projections. Interestingly, recent evidence has suggested that molecular mimicry may trigger autoimmune responses against proteins expressed in central vagal nuclei, including the nucleus ambiguus and the dorsal motor nucleus of the vagus, potentially contributing to autonomic dysfunction in Long-COVID. Although our findings do not directly address central nervous system involvement, they are consistent with the hypothesis that dysfunction of the vagal axis may occur at multiple anatomical levels [29].

Table 2
Quantification of nerve density in the skin and gastric mucosa.

Subject	Diagnosis	Age	Sex	IENF (ff/mm)	Fundus PGP innervation (nm/μm³)		Fundus VIP Innervation (nm/μm³)		Antrum PGP innervation (nm/μm³)		Antrum VIP Innervation (nm/μm³)	
CT1	Control	62	M	6.4	4.0	(0.9)	4.3	(2.1)	2.3	(0.8)	0.7	(0.2)
CT2	Control	38	M	16.1	5.6	(1.6)	2.1	(0.2)	3.9	(2.6)	1.5	(1.9)
CT3	Control	51	M	7.1	3.6	(1.1)	2.5	(1.5)	1.8	(0.5)	1.2	(1.1)
CT4	Control	24	M	13.2	3.9	(1.2)	1.3	(0.5)	3.9	(0.5)	0.4	(0.4)
CT5	Control	55	F	11.6	[b]		[b]		5.2	(0.4)	2.6	(0.2)
CT6	Control	59	M	4.9	3.3	(1.1)	1.5	(0.3)	[b]		[b]	
CT7	Control	85	F	9.2	3.7	(1.4)	2.2	(0.1)	4.3	(3.9)	4.2	(5.6)
CT8	Control	60	F	[a]	5.8	(0.7)	6.1	(0.2)	2.3	(0.3)	5.2	(0.6)
PT1	Long-COVID-19	75	F	12.5	0.9	(0.8)	0.4	(0.4)	1.5	(1.3)	0.3	(0.5)
PT2	Long-COVID-19	54	F	10.4	2.0	(1.4)	0.1	(0.1)	1.9	(1.4)	1.1	(0.5)
PT3	Long-COVID-19	73	F	13.7	4.1	(2.3)	0.1	(0.0)	1.6	(0.9)	0.4	(0.2)
PT4	Long-COVID-19	50	M	7.4	0.4	(0.4)	1.5	(0.6)	1.6	(0.4)	0.5	(0.3)
PT5	Long-COVID-19	88	M	4.5	0.5	(0.5)	0.6	(0.2)	2.0	(1.0)	0.7	(0.1)
PT6	Long-COVID-19	33	M	7.6	3.0	(1.5)	1.1	(0.1)	3.0	(1.8)	1.3	(0.5)
PT7	Long-COVID-19	39	M	5.6	2.1	(0.1)	1.6	(0.0)	3.2	(1.3)	1.8	(0.3)
PT8	Long-COVID-19	59	M	4.3	2.7	(3.2)	1.4	(1.5)	2.8	(1.9)	4.6	(3.6)
PT9	Long-COVID-19	55	F	12.4	1.0	(0.3)	1.8	(1.3)	1.2	(0.3)	0.8	(0.6)
PT10	Long-COVID-19	59	F	5.4	2.9	(1.0)	1.6	(1.3)	2.4	(0.7)	1.3	(0.2)
PT11	Long-COVID-19	38	F	16.8	1.0	(0.0)	1.2	(1.1)	1.2	(0.4)	0.9	(0.1)
PT12	Long-COVID-19	55	M	6.9	3.5	(1.4)	1.5	(0.7)	2.4	(1.0)	1.5	(0.8)
Controls		54.3 ± 17.9	5 M/3F	9.8 ± 4.0	3.9 (1.1)		2.2 (1.6)		3.9 (1.8)		1.5 (2.4)	
Long-COVID-19		56.5 ± 16.2	6 M/6F	8.9 ± 4.1	2.1 (2.0)		1.3 (0.9)		1.9 (1.0)		1.0 (0.8)	
P		>0.05	>0.05	>0.05	<0.01		<0.01		<0.05		<0.01	

The innervation data are expressed as medians and interquartile ranges (in parentheses), except for age and IENF, which are expressed as the means±standard deviations.
[a] Subject CT8 refused skin biopsy at Leg.
[b] Quality of samples from subject CT5 (fundus) and CT6 (antrum) was not sufficient for processing.CT = control; PT = patient.

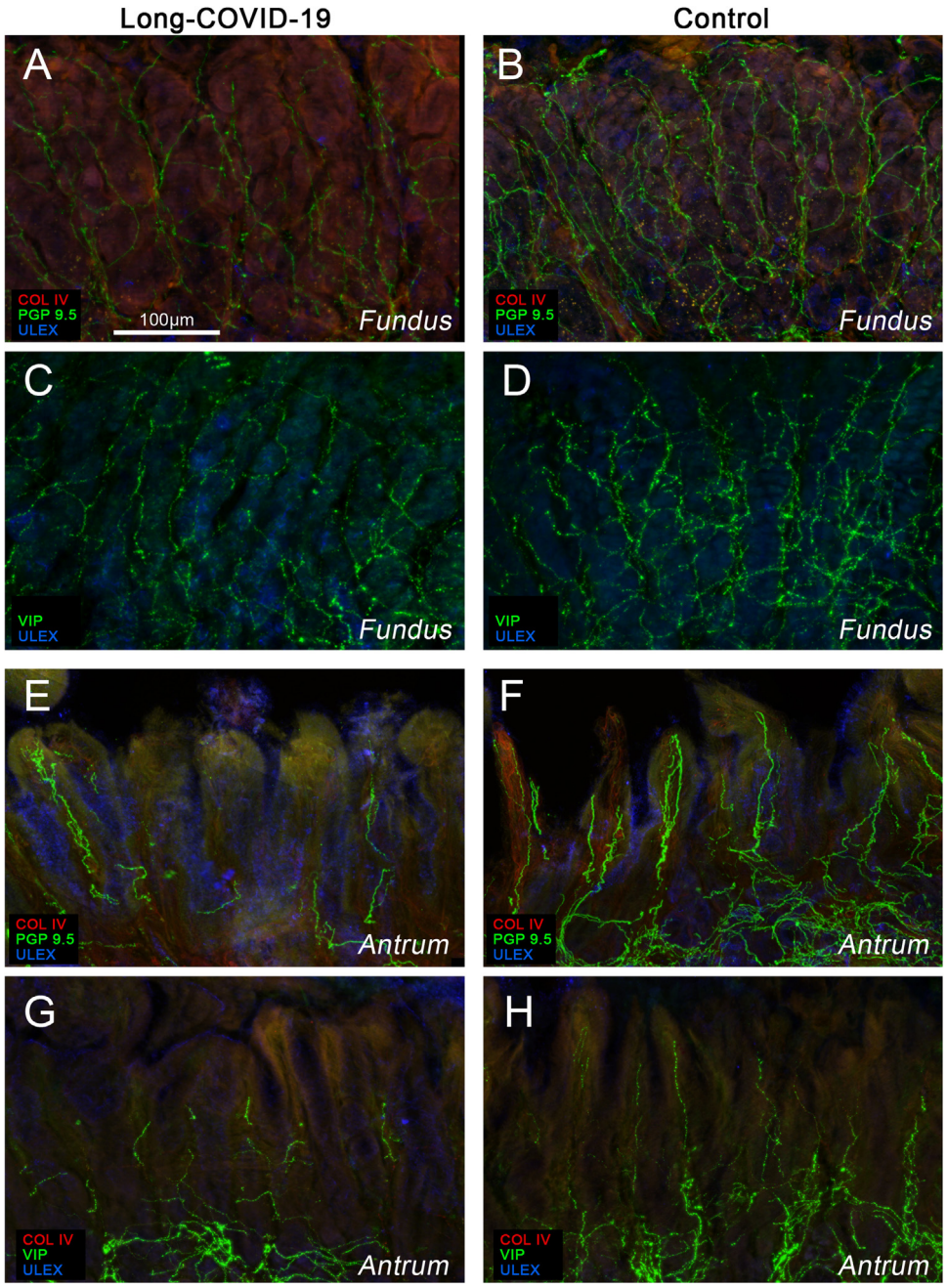


Figure 1. Gastric mucosa denervation in Long-COVID-19 patients. The panel shows gastric mucosa denervation in Long-COVID-19 patients (fundus in A and C and antrum in E and G) compared to Controls (fundus in B and D and antrum in F and H). Evident loss of PGP-ir fibers (green) in A and E (compared to B and F) and of VIP-ir fibers (green) in C and G (compared to D and H) demonstrating severe denervation in Long-COVID-19 patients involving pan- and cholinergic autonomic innervation compared to Controls. Red indicates the thin collagen layer around the glandular structures, and blue indicates the internal epithelial component.

From a pathophysiological perspective, these findings support a model in which SARS-CoV-2-related injury to vagal fibers leads to a disruption of the cholinergic anti-inflammatory pathway. Such disruption may result in a failure to adequately regulate immune responses, thereby sustaining a pro-inflammatory state and contributing to the persistence of symptoms. In this framework, the gastrointestinal tract given its extensive vagal innervation and its role as a major immunological interface may represent a critical site of pathological interaction.

Our findings support an overall parasympathetic impairment in Long-COVID-19 patients.

In our study, the loss of nerve fibers in the gastric mucosa of patients with Long-COVID-19 was not associated with cutaneous loss of somatic fibers, suggesting that in these patients, gastric mucosa denervation might be the effect of a more selective pathogenic mechanism affecting primarily the autonomic nervous system. The selectivity of a parasympathetic involvement is also suggested by the evidence of an impairment of gastric motility and a normal sudomotor function in post-COVID-19 patients [30].

A clear understanding of the pathogenetic mechanisms may be helpful in the management of Long-COVID-19, which remains a medical challenge and a public health problem since it affects 5-10% of individuals with acute SARS-CoV-2 infection. Among the different pathogenetic hypotheses, some evidence points to early and persistent involvement of the VN that may underlie several symptoms. The VN innervates the larynx, pharynx, lungs, heart, and

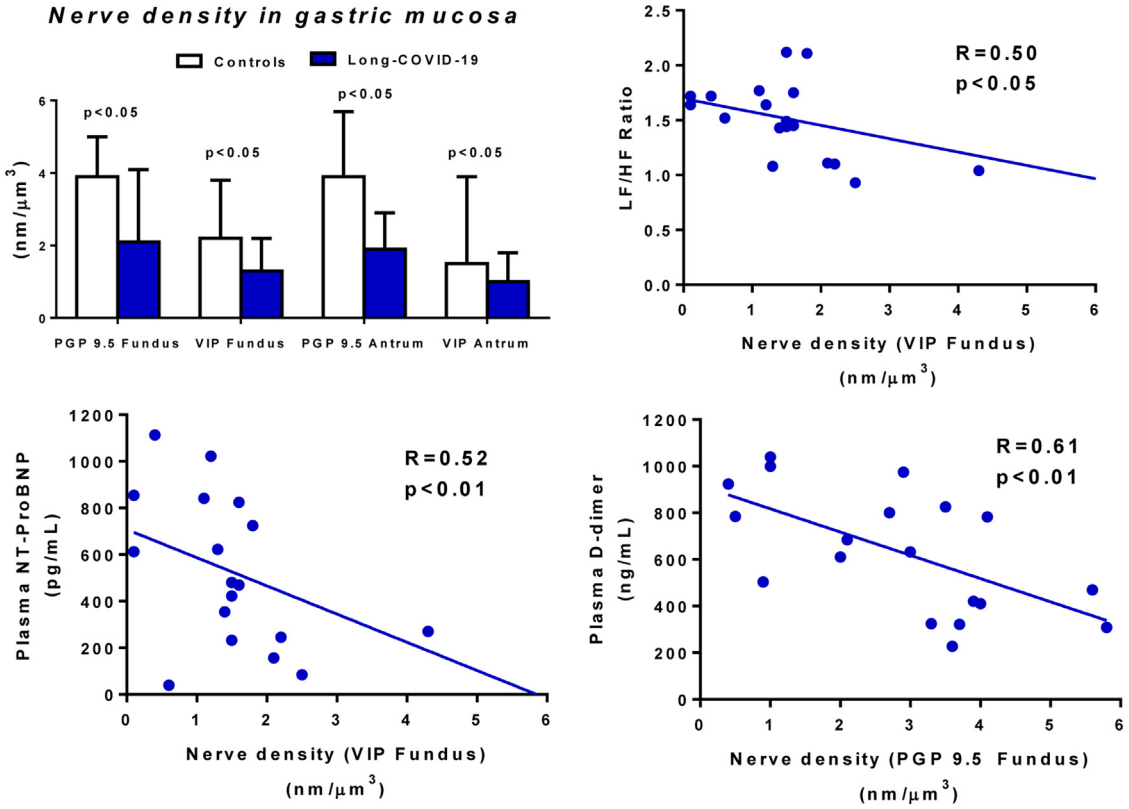


Figure 2. In A quantification of nerve density in gastric mucosa. Nerve length per volume of tissue (nm/µm3) was calculated for PGP and VIP fibers in fundus and antrum for patients and controls. From B to D correlations between nerve density and HRV, NT-proBNP and D-dimer levels.

Table 3
Heart rate variability by 24 h ECG monitoring in Controls and Long-COVID-19 patients.

	Controls	Long-COVID-19	P
Heart rate variability (time domain)			
SDNN (msec)	109.0 ± 24.1	80.3 ± 21.0	<0.05
SDANN (msec)	91.0 ± 22.0	70.6 ± 19.4	>0.05
SDNNi	55.5 ± 11.2	32.9 ± 10.8	<0.01
rMSSD (msec)	48.5 ± 26.7	15.3 ± 5.4	<0.01
pNN50 (%)	18.8 ± 13.0	0.8 ± 1.5	<0.01
Heart rate variability (spectral power)			
Total power (ln msec^2)	8.2 ± 0.4	7.1 ± 0.4	<0.01
VLF (ln msec^2)	7.6 ± 0.4	6.5 ± 0.6	<0.01
LF (ln msec^2)	6.5 ± 0.6	6.4 ± 0.4	>0.05
HF (ln msec^2)	5.8 ± 0.9	3.8 ± 0.5	<0.01
LF/HF ratio	1.1 ± 0.1	1.7 ± 0.2	<0.01

Data are expressed as Mean ± standard deviation.
HF = high-frequency component; LF = low-frequency component; ln = logarithm; pNN50 = percentage of difference between adjacent normal R-R intervals that is greater than 50 ms computed over the entire 24-h ECG recording; rMSSD = square root of the mean of the sum of the squares of differences between adjacent R-R intervals; SDANN = standard deviation of the averages of R-R intervals in all 5 min segments of the entire recording; SDNN = standard deviation of all R-R intervals; SDNNi = mean of the standard deviations of all R-R intervals for all 5 min segments of the entire recording; VLF = very-low-frequency component.

gastrointestinal tract. The GI tract is the second-largest interface between the external environment and the body and is continuously vulnerable to potentially damaging agents and pathogens. In particular, in the stomach, the VN acts as a sensory afferent and efferent pathway to sense injury and to apply protective strategies controlling involuntary visceral functions as part of the autonomic nervous system and modulating systemic inflammation. In particular, the role of gastric vagal innervation is essentially protective. It signals potential threats to the central nervous system at the gastrointestinal level, eliciting autonomic, emotional-affective and neuroendocrine reactions [31]. So, a disruption of vagal innervation may underlie persistent symptoms after SARS-CoV-2 infection.

Histological evidence of VN involvement has recently been provided through the demonstration of inflammatory cell infiltration during SARS-CoV-2 infection [30].

Although we are not able to discriminate between intrinsic and extrinsic parasympathetic gastric innervation, our data support the hypothesis that the axonal damage to vagal fibers induced by SARS-CoV-2 trafficking along nerve fibers leads to autonomic dysfunction and a lack of VN-mediated inhibition of proinflammatory mechanisms in Long-COVID-19 patients.

This model is in agreement with recent morphological and functional findings of VN impairment based on neck ultrasound observations of increased echogenicity in the epineurium, focal thickening of the nerve and reduced gastrointestinal motility [31].

The clinical implications of these findings are substantial. The identification of a structural autonomic substrate opens new avenues for targeted therapeutic strategies aimed at restoring vagal function or enhancing cholinergic signaling. Interventions such as vagus nerve stimulation or pharmacological modulation of cholinergic pathways may therefore represent promising approaches for the management of Long-COVID-19, although further studies are needed to evaluate their efficacy.

Limitations

This study has several limitations. First, it is a single-center proof-of-concept study with a relatively small sample size, which may limit the generalizability of the findings. So further studies based on larger population of patients and controls are warranted. However, the strict inclusion criteria and the invasive nature of the procedures required for tissue acquisition make the recruitment of larger cohorts challenging.

Second, the control group consisted of patients undergoing endoscopy for dyspeptic symptoms rather than completely healthy individuals, which may introduce potential bias. Nevertheless, no macroscopic or histological abnormalities were observed in the gastric mucosa, supporting their suitability as controls.

Third, we did not include patients who recovered from SARS-CoV-2 infection without persistent symptoms, which would have provided additional insight into the specificity of the observed alterations.

Finally, our methodological approach does not allow discrimination between intrinsic enteric and extrinsic vagal cholinergic innervation or between cholinergic, and non-adrenergic non cholinergic (NANC) VIP-positive fibers. Therefore, although our findings strongly suggest vagal involvement, the precise anatomical origin of the observed denervation cannot be definitively established.

Conclusions

In conclusion, this study provides the first *in vivo* morphological evidence of gastric mucosal cholinergic denervation in patients with Long-COVID-19. The observed association between structural denervation and alterations in heart rate variability supports the presence of a structural–functional autonomic impairment, likely involving vagal pathways.

These findings identify a potential anatomical substrate for dysautonomia in Long-COVID-19 and offer a novel perspective on the pathophysiology of persistent symptoms.

Further studies are warranted to confirm these results and to explore whether targeted interventions aimed at restoring vagal function may improve clinical outcomes in this population.

Informed consent statement

Informed consent was obtained from all the subjects involved in the study.

Data availability statement

The dataset generated and analyzed during the current study is available from Dr Domenico Acanfora, Department of Internal Medicine San Francesco Hospital, Viale Europa 21, 82037 Telese Terme, Benevento, Italy; e-mail:domenico.acanfora29@gmail.com.

Declaration of competing interest

The authors declare that they have no known competing financial interests or personal relationships that could have appeared to influence the work reported in this paper.

CRediT authorship contribution statement

Domenico Acanfora: Conceptualization, Data curation, Formal analysis, Investigation, Methodology, Supervision, Validation, Visualization, Writing – original draft, Writing – review & editing. **Maria Nolano:** Conceptualization, Data curation, Formal analysis, Investigation, Methodology, Resources, Supervision, Validation, Visualization, Writing – original draft, Writing – review & editing. **Chiara Acanfora:** Conceptualization, Data curation, Formal analysis, Investigation, Methodology, Resources, Supervision, Validation, Visualization, Writing – original draft, Writing – review & editing. **Camillo Colella:** Conceptualization, Data curation, Methodology, Writing – original draft, Writing – review & editing. **Vincenzo Provitera:** Conceptualization, Data curation, Formal analysis, Investigation, Methodology, Supervision, Validation, Visualization, Writing – original draft, Writing – review & editing. **Giuseppe Caporaso:** Conceptualization, Data curation, Formal analysis, Investigation, Methodology, Software, Supervision, Validation, Visualization, Writing – original draft, Writing – review & editing. **Giuseppe Rengo:** Conceptualization, Data curation, Formal analysis, Investigation, Methodology, Project administration, Supervision, Validation, Visualization, Writing – original draft, Writing – review & editing. **Raffaele Antonelli Incalzi:** Conceptualization, Data curation, Formal analysis, Investigation, Methodology, Supervision, Validation, Visualization, Writing – original draft, Writing – review & editing. **Gerardo Casucci:** Conceptualization, Data curation, Investigation, Methodology, Project administration, Supervision, Validation, Visualization, Writing – original draft, Writing – review & editing.

Funding

This research received no external funding.

Ethical approval

The study was conducted according to the guidelines of the Declaration of Helsinki and was approved by the Institutional Review Board (March 22, 2021) of the San Francesco Hospital of Telese Terme (BN).

Acknowledgments

The authors would like to thank Ada d'Aniello for the English language revision and Antonietta Ferrucci, Francesca Carangelo and Carmelina Morra for the data collection and analysis.

Supplementary materials

Supplementary material associated with this article can be found, in the online version, at doi:10.1016/j.ijid.2026.108973.

References

[1] Rabaan AA, Al-Ahmed SH, Haque S, Sah R, Tiwari R, Malik YS, et al. SARS-CoV-2, SARS-CoV, and MERS-COV: a comparative overview. *Infez Med* 2020;**28**(2):174–84.
[2] Sharma A, Tiwari S, Deb MK, Marty JL. Severe acute respiratory syndrome coronavirus-2 (SARS-CoV-2): a global pandemic and treatment strategies. *Int J Antimicrob Agents* 2020;**56**(2):106054. doi:10.1016/j.ijantimicag.2020.106054.
[3] Messlinger K, Neuhuber W, May A. Activation of the trigeminal system as a likely target of SARS-CoV-2 may contribute to anosmia in COVID-19. *Cephalalgia* 2022;**42**(2):176–80. doi:10.1177/03331024211036665.
[4] Lai CC, Ko WC, Lee PI, Jean SS, Hsueh PR. Extra-respiratory manifestations of COVID-19. *Int J Antimicrob Agents* 2020;**56**(2):106024. doi:10.1016/j.ijantimicag.2020.106024.
[5] Mariotto S, Savoldi A, Donadello K, Zanzoni S, Bozzetti S, Carta S, et al. Nervous system: subclinical target of SARS-CoV-2 infection. *J Neurol Neurosurg Psychiatry* 2020;**91**(9):1010–12. doi:10.1136/jnnp-2020-323881.

[6] Kanberg N, Ashton NJ, Andersson LM, Yilmaz A, Lindh M, Nilsson S, et al. Neurochemical evidence of astrocytic and neuronal injury commonly found in COVID-19. *Neurology* 2020;**95**(12):e1754–9. doi:10.1212/WNL.0000000000010111.
[7] Xie Z, Hui H, Zhao Z, Yu W, Wu R, Zhu Y, et al. Nervous system manifestations related to COVID-19 and their possible mechanisms. *Brain Res Bull* 2022;**187**:63–74. doi:10.1016/j.brainresbull.2022.06.014.
[8] Carod-Artal FJ, García-Moncó JC. Epidemiology, pathophysiology, and classification of the neurological symptoms of post-COVID-19 syndrome. *Neurol Perspect* 2021;**1**:S5–S15. doi:10.1016/j.neurop.2021.07.005.
[9] Achar A, Ghosh C COVID-19-associated neurological disorders: the potential route of CNS invasion and blood-brain relevance. Cells 27;9(11):2360. doi: 10.3390/cells9112360.
[10] Fenrich M, Mrdenovic S, Balog M, Tomic S, Zjalic M, Roncevic A, et al. SARS-CoV-2 dissemination through peripheral nerves explains multiple organ injury. *Front Cell Neurosci* 2020;**14**:229. doi:10.3389/fncel.2020.00229.
[11] Douaud G, Lee S, Alfaro-Almagro F, Arthofer C, Wang C, McCarthy P, et al. SARS-CoV-2 is associated with changes in brain structure in UK Biobank. *Nature* 2022;**604**(7907):697–707. doi:10.1038/s41586-022-04569-5.
[12] Tornero C, Pastor E, Garzando MDM, Orduña J, Forner MJ, Bocigas I, et al. Non-invasive vagus nerve stimulation for COVID-19: results from a randomized controlled trial (SAVIOR I). *Front Neurol* 2022;**13**:820864. doi:10.3389/fneur.2022.820864.
[13] Acanfora D, Nolano M, Acanfora C, Colella C, Provitera V, Caporaso G. Impaired vagal activity in long-COVID-19 patients. *Viruses* 2022;**14**(5):1035. doi:10.3390/v14051035.
[14] Bonaz B, Sinniger V, Pellissier S. The vagus nerve in the neuro-immune axis: implications in the pathology of the gastrointestinal. *Front Immunol* 2017;**8**:1452. doi:10.3389/fimmu.2017.01452.
[15] Ayoubkhani D, Khunti K, Nafilyan V, Maddox T, Humberstone B, Diamond I, et al. Post-covid syndrome in individuals admitted to hospital with covid-19: retrospective cohort study. *BMJ* 2021;**372**:n693. doi:10.1136/bmj.n693.
[16] DeVries A, Shambhu S, Sloop S, Overhage JM. One-year adverse outcomes among US adults with Post-COVID-19 condition vs those without COVID-19 in a large commercial insurance database. JAMA Health Forum. 2023;3;4(3):e230010. Doi: 10.1001/jamahealthforum.2023.0010. Erratum in. *JAMA Health Forum* 2023;**4**(7):e232428. doi:10.1001/jamahealthforum.2023.2428.
[17] Donadio V, Nolano M, Provitera V, Stancanelli A, Lullo F, Liguori R, et al. Skin sympathetic adrenergic innervation: an immunofluorescence confocal study. *Ann Neurol* 2006;**59**(2):376–81. doi:10.1002/ana.20769.
[18] Nolano M, Provitera V, Perretti A, Stancanelli A, Saltalamacchia AM, Donadio V, et al. Ross syndrome: a rare or a misknown disorder of thermoregulation? A skin innervation study on 12 subjects. *Brain* 2006;**129**(8):2119–31. doi:10.1093/brain/awl175.
[19] Parisi V, Rengo G, Perrone-Filardi P, Pagano G, Femminella GD, Paolillo S, et al. Increased epicardial adipose tissue volume correlates with cardiac sympathetic denervation in patients with heart failure. *Circ Res* 2016;**118**(8):1244–53. doi:10.1161/CIRCRESAHA.115.307765.
[20] Acanfora D, Casucci G, Ciccone MM, Scicchitano P, Lonobile T, Chiariello L, et al. Pathological evidence of adrenergic cardiac denervation in a patient with congestive heart failure. *Cardiovasc Pathol* 2018;**36**:20–1. doi:10.1016/j.carpath.2018.05.007.
[21] Selim MM, Wendelschafer-Crabb G, Redmon JB, Khoruts A, Hodges JS, Koch K, et al. Gastric mucosal nerve density: a biomarker for diabetic autonomic neuropathy? *Neurology* 2010;**75**(11):973–81. doi:10.1212/WNL.0b013e3181f25f19.
[22] Shah W, Hillman T, Playford ED, Hishmeh L. Managing the long term effects of covid-19: summary of NICE, SIGN, and RCGP rapid guideline. BMJ 2021;22;372:n136. Doi: 10.1136/bmj.N136. Erratum in. *BMJ* 2022;**19**:o126. doi:10.1136/bmj.o126.
[23] Heart rate variability: standards of measurement, physiological interpretation and clinical use. Task Force of the European Society of Cardiology and the North American Society of Pacing and Electrophysiology. *Circulation* 1996;**93**(5):1043–65.
[24] Takabatake N, Nakamura H, Minamihaba O, Inage M, Inoue S, Kagaya S, et al. A novel pathophysiologic phenomenon in cachexic patients with chronic obstructive pulmonary disease: the relationship between the circadian rhythm of circulating leptin and the very low-frequency component of heart rate variability. *Am J Respir Crit Care Med* 2001;**163**(6):1314–19. doi:10.1164/ajrccm.163.6.2004175.
[25] Vinik AI, Ziegler D. Diabetic cardiovascular autonomic neuropathy. *Circulation* 2007;**115**(3):387–97. doi:10.1161/CIRCULATIONAHA.106.634949.
[26] Provitera V, Iodice V, Manganelli F, Mozzillo S, Caporaso G, Stancanelli A, et al. Postganglionic sudomotor assessment in early stage of multiple system atrophy and Parkinson Disease: a morpho-functional study. *Neurology* 2022;**98**(12):e1282–91. doi:10.1212/WNL.0000000000013300.
[27] Lauria G, Hsieh ST, Johansson O, Kennedy WR, Leger JM, Mellgren SI, et al. European Federation of Neurological Societies/Peripheral Nerve Society guideline on the use of skin biopsy in the diagnosis of small fiber neuropathy. Report of a joint task force of the European Federation of Neurological Societies and the Peripheral Nerve Society. *Eur J Neurol* 2010;**17**(7):903–12 e44–9. doi:10.1111/j.1468-1331.2010.03023.x.
[28] Anetsberger D, Kürten S, Jabari S, Brehmer A. Morphological and immunohistochemical characterization of Human intrinsic gastric neurons. *Cells Tissues Organs* 2018;**206**(4–5):183–95. doi:10.1159/000500566.
[29] D'Anna SE, Vitale AM, D'Amico G, Caruso Bavisotto C, Ambrosino P, Cappello F, et al. Autoimmunity against nucleus ambiguous is putatively possible in both long-COVID-19 and vaccinated subjects: scientific evidence and working hypothesis. *Biology* 2024;**13**:359. doi:10.3390/biology13060359.
[30] Woo MS, Shafiq M, Fitzek A, Dottermusch M, Altmeppen H, Mohammadi B, et al. Vagus nerve inflammation contributes to dysautonomia in COVID-19. *Acta Neuropathol* 2023;**146**(3):387–94. doi:10.1007/s00401-023-02612-x.
[31] Lladós G, Massanella M, Coll-Fernández R, Rodríguez R, Hernández E, Lucente G, et al. Vagus nerve dysfunction in the post-COVID-19 condition: a pilot cross-sectional study. *Clin Microbiol Infect* 2024;**30**(4):515–21. doi:10.1016/j.cmi.2023.11.007.